ISSN 1063-7729, Astronomy Reports, 2022, Vol. 66, No. 12, pp. 1312–1318. © Pleiades Publishing, Ltd., 2022.
Russian Text © The Author(s), 2022, published in Astronomicheskii Zhurnal, 2022, Vol. 99, No. 12, pp. 1264–1271.

Use of Generalized Exponential Functions in the Analysis of Statistical Characteristics of Interstellar Scintillations of Pulsars

M. V. Popov*

Astrospace Center, Lebedev Physical Institute, Russian Academy of Sciences, Moscow, 117485 Russia

**e-mail: popov069@asc.rssi.ru*

Received October 9, 2022; revised October 20, 2022; accepted October 24, 2022

Abstract—It is proposed to approximate the frequency and time sections of the two-dimensional autocorrelation functions of the dynamic spectra of pulsar scintillations by a universal exponential function with an arbitrary exponent m. This approximation describes the shape of the correlation function much better than the Gaussian or simple exponential function. The relationship between the shape of autocorrelation functions and the initial profile of the average frequency structure of diffractive scintillations is studied by numerical simulation. It is shown that the true width of this average frequency profile differs significantly from the width of the autocorrelation function, which leads to a shift in estimates of some effects caused by scintillations. Examples of such distorted estimates for the pulsar velocity (V_{iss}) and for the transition from the decorrelation bandwidth Δf to the scattering time $\Delta\tau_s$ are presented.

Keywords: pulsars, scattering of radio emission by interstellar plasma

DOI: 10.1134/S1063772922110166

1. INTRODUCTION

The sizes of the pulsar radio emission region cannot exceed the sizes of the magnetosphere of a neutron star, limited by a light cylinder with a radius $R_L = Pc/2\pi$, which, for a pulsar pulse repetition period P of one second, will be about 5×10^9 cm. The angular size of such a region with a typical distance to pulsars of several hundred parsecs turns out to be less than an angular microsecond. In fact, the sizes R_{em} of the radio emission region are much smaller than the sizes of the light cylinder: with a typical duration δt of pulsar subpulses of several milliseconds, $R_{\text{em}} \approx c\delta t = 3\times10^7$ cm. Thus, pulsars are point radio sources that are convenient for studying the effects of radio emission scattering by interstellar plasma inhomogeneities, since there is no need to consider the structure of the radio emission source. Therefore, intensive studies of scattering effects began precisely after the discovery of pulsars. The main theoretical concepts can be found in the review article by Rickett [1]. The main scattering parameters are the characteristic scintillation time t_{scint}; the pulse scattering time $\Delta\tau_s$; the frequency scale of the diffraction distortion of the radio spectrum Δf, called the decorrelation band; and the apparent angular expansion of the source, θ_{sc}. To estimate the scattering parameters t_{scint} and Δf, the dynamic spectra are usually analyzed over the time interval $T_{\text{obs}} > t_{\text{scint}}$, in order to achieve some statistical significance [2–4]. On this observational interval, two-dimensional correlation functions (ACFs) of the dynamic spectra are calculated. The details of the calculation and normalization of the ACF are given in the above-cited publications [2–4]. The pulse scattering time $\Delta\tau_s$ is determined by analyzing the shape of the average pulse profile (see, e.g., Kuzmin and Losovsky [5]). Such "direct" measurements of $\Delta\tau_s$ are possible for pulsars with a large dispersion and/or at low radio frequencies, where the scattering time exceeds a few microseconds. Smaller values of $\Delta\tau_s$ are obtained by converting from the measured decorrelation band Δf via the uncertainty relation $2\pi\Delta\tau_s\Delta f = 1$; the limitations of this method will be considered in Section 4.2. In Section 2, we formulate the basic premises for further analysis; then, in Section 3, we present the results of numerical simulation of the main types of autocorrelation functions and establish the relation between their parameters. In Section 4, we compare our results with observational data.

2. INITIAL PREMISES

The apparent angular expansion of a source, θ_{sc}, is measured using very long baseline interferometry

(VLBI). Great progress in this area was achieved during the implementation of the Radioastron ground-space interferometer project [6]. Some results of such measurements were considered by Popov et al. in [7]. In this work, the form of the interferometric response as a function of the time delay (amplitude of the visibility function $V(\tau)$) was analyzed. It turned out that the averaged autocorrelation function of the visibility is well described by the Lorentzian function $\mathrm{ACF}(V(\tau)) = L(\delta\tau) = A_l/(\delta\tau^2 + d^2)$, where the parameter d is the half width of this function at a level of 1/2 and A_l is the scale factor. Here, we introduce several mathematical relations useful for further presentation. We write an expression for the Lorentzian function:

$$L(d,t) = A_l/(t^2 + d^2). \tag{1}$$

The autocorrelation function for the Lorentzian function is given by the formula

$$\mathrm{ACF}[L(d,t)] = L(2d,\Delta t), \tag{2}$$

i.e., the FWHM of the autocorrelation function is twice the FWHM of the function itself. The Fourier transform of the Lorentzian function is a two-sided exponential function

$$FT(L(d,t)) = A_F \exp(-2\pi d\,|x|). \tag{3}$$

Here, the half width of the function FT at a level of $1/e$ is $W^F_{1/e} = 1/(2\pi d)$; therefore, in this case, the uncertainty relation $2\pi W^F_{1/e} W^L_{1/2} = 1$ is satisfied exactly. As noted above, according to the analysis by Popov et al. [7], the ACF of the visibility function $V(\tau)$ for all studied pulsars is well approximated by the Lorentzian function. In accordance with expression (2), the visibility function $V(\tau)$ also must be described by the Lorentzian function. The visibility function $V(\tau)$ is obtained as the inverse Fourier transform of the cross-correlation spectrum $S(f)$; i.e., $V(\tau) = FT^{-1}(S(f))$. Therefore, in accordance with Eq. (3), the average structure of the cross-correlation (or autocorrelation) spectrum is a set of two-sided exponentials. Unlike the average pulse profile of a pulsar, it is not possible to accumulate the average profile of the frequency diffraction structure, since this structure changes with time randomly, which is the scintillation phenomenon. However, it is possible to immediately accumulate the autocorrelation function of the scintillation frequency structure or the two-dimensional ACF from the dynamic spectra for measuring the time and frequency sections. This approach was used by many researchers (see, e.g., [2–4]. In this case, the time and frequency sections of the ACF were approximated by Gaussians. Other researchers using correlation functions for data analysis [8–10] pointed out the deviations of these functions from the Gaussian form. According to the concepts outlined above, the frequency cross section of the ACF must correspond to the autocorrelation function of a two-sided exponential:

$$E(b,f) = A_e \exp\left(-\frac{|f|}{b}\right). \tag{4}$$

This function has already been declared in relation (3). The ACF of the two-sided exponential is

$$\mathrm{ACF}(E(b,f)) = A_{\mathrm{ACF}}(|\delta f| + b)\exp\left(-\frac{|\delta f|}{b}\right), \tag{5}$$

which we will call the modified exponent; here, A_{ACF} is the scale factor and b is the half width of the original exponent at a level of $1/e$. However, the half width of the autocorrelation function $\mathrm{ACF}(E(b,f))$ is by no means equal to b, but exceeds it more than two-fold! Algebraic expressions (1)–(5) were borrowed from Feller's monograph [11]. In the article [12], Popov and Smirnova analyzed the time cross sections of two-dimensional ACFs for several pulsars. It was found that Gaussians are not suitable for approximating time sections. It was proposed to use a universal exponential function of the form

$$U(\nu) = A_u \exp\left(-\frac{|\nu|^m}{b}\right), \tag{6}$$

where A_u is the scale factor and the half width of $U(\nu)$ is determined from the relation $W^U_{1/e} = b^{1/m}$. For the time sections of the ACF, Popov and Smirnova [12] showed that the exponent m can be related to the exponent n of the spatial spectrum of interstellar plasma inhomogeneities, which is described by the relation $F_n(q) = Cq^{-n}$, where q is the spatial frequency and C is the structural constant. This relation is defined by a simple equality $n = m + 2$. We performed an approximation by the universal function (6) of the frequency cross sections of two-dimensional correlation functions according to the data used in [12]. A summary of exponents m for time and frequency sections will be given below. For frequency sections, no simple relation of the exponent m with the exponent n of the spatial spectrum of inhomogeneities was proposed. In this article, we will use the universal exponential function $U(\nu)$ to simulate the shape of an averaged frequency structure in order to establish a relation between frequency functions and their autocorrelations. This function has no obvious physical meaning, but it has the property of well approximating bell curves due to the presence of three free parameters A, b, and m.

3. NUMERICAL SIMULATION OF AUTOCORRELATION FUNCTIONS

As already mentioned in the Introduction, during the analysis of observational data (dynamic spectra),

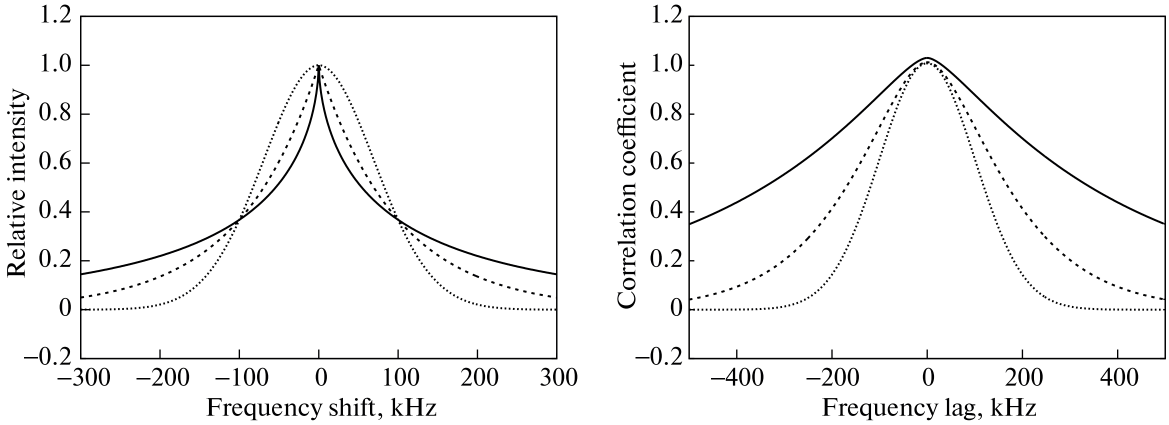

Fig. 1. (Left) Comparison of the synthesized average frequency distortion profiles and (right) the shape of the corresponding autocorrelation functions: (dashed line) the spectral profile $U(\nu)$ is defined by a two-sided exponential ($m_0 = 1.0$); (dotted line) Gaussian frequency profile; (solid line) autocorrelation function in the form of a pure exponential.

two-dimensional correlation functions (ACF) averaged over a time T_{obs} significantly exceeding the characteristic scintillation time t_{scint} are calculated. From the time and frequency cross sections of these ACFs, important scintillation parameters are obtained. However, as already shown in the previous section, the half width of the autocorrelation function does not coincide with the half width of the original function inherent in the scattering process. It is impossible to obtain the shape of this initial function from the observed ACF cross section (deconvolution) without preconditions. Therefore, in our numerical simulation, the initial signal was specified as the average profile of the scintillation frequency structure in the form a function $U(\nu)$ with different exponents m_0 and then the corresponding autocorrelation functions were calculated as a convolution:

$$A(\Delta\nu) = \frac{1}{B - \Delta\nu} \int_0^{B-\Delta\nu} U(\nu)U(\nu + \Delta\nu)d\nu. \quad (7)$$

Here, B is the spectral interval on which the function $U(\nu)$ is defined. In fact, the integral in expression (7) was determined by calculating the sum of products on this frequency interval B. For clarity, we point out that the half width of all model functions was the same and was taken equal to 100 kHz and the spectral interval was 32.768 MHz (N2768). These details are necessary for the conversion to the visibility function $V(\tau)$.

Thus, the initial functions $U(\nu)$ define the average shape of the diffraction frequency (or time) distortions of the radio spectrum of the pulsar. These functions are real and even. They imitate the structure of the power spectrum under the assumption that there is a certain average frequency profile of spectral distortions, which is confirmed by the existence of stable and repetitive shapes of averaged ACF of the dynamic spectra. The natural condition always accepted was that this average frequency profile is described by a Gaussian function. Then, the ACF of the dynamic spectra would also have a Gaussian shape. In practice, there is a wide variety of the shapes of averages. Our analysis is purely mathematical. The initial functions $U(\nu)$ do not contain any noise components. The simulation results are presented in Table 1. The first column gives the exponent m_0 of the function $U(\nu)$; the second column gives the exponents m_1 of the autocorrelation function $A(\Delta\nu)$ approximated by the universal exponential function $U(\Delta\nu)$; the third column contains the exponent m_2 obtained as a result of the approximation of the visibility function $V(\tau)$ calculated via the inverse Fourier transform of the initial function $U(\nu)$: $V(\tau) = FT^{-1}(U(\nu))$. The temporal resolution of the visibility function for our conditions is $\delta\tau = 1/B = 0.0305\,\mu s$. The fourth column gives the factor R of the increase in the half width of the autocorrelation function $A(\Delta\nu)$ with respect to the half width of the initial function $U(\nu)$. In the fifth column, we give the values of the half width of the visibility function and, in the last two columns, the values of the product $2\pi\Delta\nu\Delta\tau$, K_1, and K_2. Figure 1 shows examples of model functions of the diffractive frequency structure $U(\nu)$ (left) and their corresponding autocorrelation functions $A(\Delta\nu)$ (right). The dashed line corresponds to the case when the spectral profile of the frequency structure $U(\nu)$ is given by a two-sided exponential ($m_0 = 1.0$); for such a function, the autocorrelation function is described by modified exponent (5), the half width of which is approximately 2 times greater than the half width of the frequency profile. The dotted line corresponds to the Gaussian frequency profile. It is known that the autocorrelation function of a Gaussian is also a Gaussian with a half

Table 1. Simulation results

Exponent			ACF broadening factor R	FWHM $V(\tau)$, μs	K_1	K_2
$U(\nu)(m_0)$	ACF from $U(\nu)$ (m_1)	$V(\tau)$ (m_2)				
0.45	0.77	0.61	9.32	0.197	0.124	1.155
0.50	0.84	0.67	6.87	0.298	0.187	1.284
0.55	0.91	0.73	5.42	0.415	0.261	1.414
0.60	0.98	0.80	4.48	0.552	0.346	1.515
0.65	1.05	0.87	3.80	0.689	0.433	1.662
0.70	1.11	0.94	3.38	0.836	0.525	1.744
0.75	1.17	1.01	3.04	0.976	0.613	1.863
0.80	1.22	1.08	2.77	1.113	0.699	1.936
0.85	1.28	1.16	2.56	1.241	0.780	1.997
0.90	1.33	1.23	2.40	1.363	0.856	2.054
0.95	1.38	1.30	2.26	1.476	0.929	2.099
1.00	1.43	1.36	2.15	1.560	0.992	2.133
1.05	1.48	1.43	2.05	1.678	1.054	2.161
1.10	1.52	1.49	1.97	1.766	1.109	2.185
1.15	1.56	1.54	1.90	1.848	1.161	2.206
1.20	1.60	1.60	1.84	1.928	1.211	2.228
1.25	1.64	1.64	1.78	1.998	1.255	2.234
1.30	1.67	1.69	1.74	2.062	1.295	2.253
1.35	1.71	1.73	1.70	2.126	1.336	2.271
1.40	1.74	1.77	1.66	2.181	1.370	2.274
1.45	1.77	1.80	1.63	2.236	1.404	2.288
1.50	1.80	1.83	1.60	2.284	1.435	2.296
1.55	1.83	1.86	1.57	2.330	1.464	2.298
1.60	1.85	1.88	1.55	2.376	1.493	2.314
1.65	1.88	1.90	1.53	2.416	1.518	2.328
1.70	1.90	1.92	1.52	2.455	1.542	2.434
1.75	1.92	1.94	1.49	2.489	1.564	2.330
1.80	1.94	1.95	1.47	2.525	1.587	2.333
1.85	1.96	1.97	1.46	2.556	1.606	2.344
1.90	1.97	1.98	1.44	2.586	1.625	2.340
1.95	1.99	1.99	1.43	2.614	1.642	2.348
2.00	2.00	2.00	1.41	2.641	1.660	2.349

width $\sqrt{2}$ times greater than the original half width. Finally, the third example, shown by a solid line, corresponds to the case when the autocorrelation function has the form of a pure exponential. Such an autocorrelation function corresponds to a frequency profile in the form of a modified zero-order Bessel function of the second kind, formally tending to infinity at zero bias [11]. In our numerical simulation, closest to this case is the variant with the exponents $m_0 = 0.60$ and $m_1 = 0.98$. It is this case that is shown in Fig. 1 by a solid line, so that the autocorrelation function does not look like a pure exponential and the frequency profile function does not tend to infinity.

Figure 2 shows the dependence of the factor R, which determines the broadening of the autocorrelation function with respect to the original function of the profile of the frequency diffraction structure, on the exponent m of the universal exponential function approximating the given ACF. In some cases, this factor indicates a tenfold broadening, and, in minimal cases, it turns out to be about 1.4.

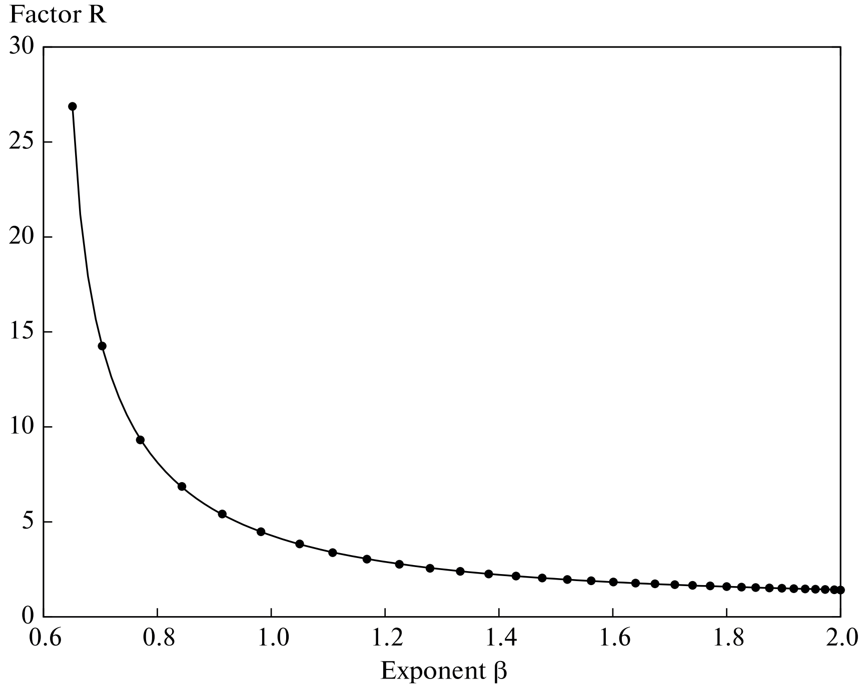

Fig. 2. Factor R characterizing the ACF expansion relative to the initial width of the scintillation process vs. the exponent m_l in the approximation of the ACF by the universal exponential function $U(x)$.

4. COMPARISON WITH OBSERVATIONAL DATA

We begin the comparison with observational data with considering Table 2, which presents the measured exponents β determined from the cross sections of two-dimensional autocorrelation functions for 11 pulsars presented in [12]. With regard to the frequency structure, the minimum value of the exponent m_l was found for the B0823+26 pulsar (m_l = 0.76), which corresponds to an almost 10-fold broadening of the ACF. The maximum (threefold) broadening of the ACF of the cross section in time is observed for the B1933+16 pulsar (m_l = 1.18). Although the statistics from a dozen pulsars cannot be considered convincing, we still present the average values of the ACF broadening in frequency and time, which amounted to 3.0 and 2.0, respectively, with a reliability of 30%. We will use this estimate in the next section.

Table 2. Summary of the results of measurements of exponents of the universal exponential function

Pulsar	Exponent	
	m_f	m_t
B0329+54	1.14	1.67
B0525+21	1.11	—
B0809+74	—	1.33
B0823+26	0.76	1.66
B0834+06	1.11	1.53
B0919+06	0.83	1.57
B1133+16	1.45	1.86
B1237+16	1.47	1.39
B1749–28	1.26	1.82
B1929+10	1.26	1.65
B1933+16	0.98	1.18
B2016+28	1.38	1.36

4.1. Scintillation Rates

In 1986, Cordes [3] published a large paper devoted to the determination of space velocities for 71 pulsars, based on measurements of the scintillation parameters Δf and $t_{\rm scint}$. These quantities were determined by the author from the time and frequency cross sections of two-dimensional autocorrelation functions using the Gaussian approximation. The main expression by which the spatial velocities were calculated is

$$V_{\rm iss} = A_V \frac{\sqrt{\Delta f D_{\rm kpc}}}{(\nu_{\rm GHz} t_{\rm scint})}. \quad (8)$$

Since the parameters Δf and $t_{\rm scint}$ were determined from autocorrelation functions, their values turned out to be overestimated 3-fold for Δf and 2-fold for $t_{\rm scint}$. When converting to real values Δf and $t_{\rm scint}$, estimates

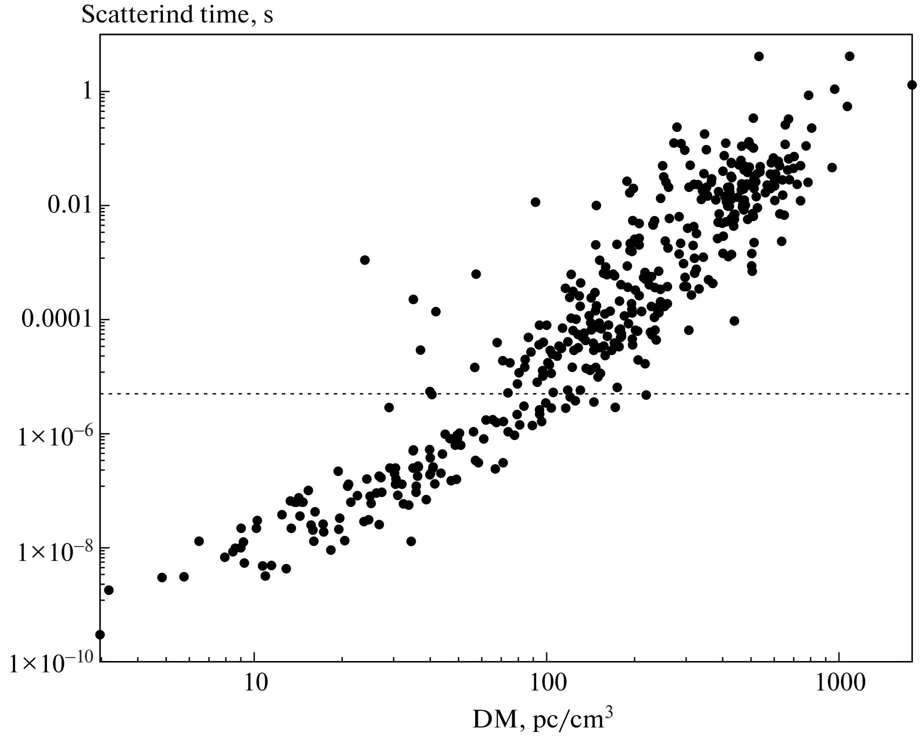

Fig. 3. Pulse broadening $\Delta\tau_s$ at a frequency of 1 GHz vs. the dispersion according to the data of the pulsar catalog [16]. The dotted line corresponds to $\Delta\tau_s = 10\,\mu s$. Greater values of $\Delta\tau_s$ were determined from pulse broadening measurements, and smaller values were obtained by recalculation from Δf.

should be corrected by a factor of $2/\sqrt{3} = 1.15$. In this case, the correction factors in the numerator and denominator of the fraction compensated each other and the velocity estimates in [3] can be considered consistent.

4.2. Uncertainty Relation

When comparing the parameters Δf and $\Delta\tau_s$, the uncertainty relation $2\pi\Delta f\Delta\tau_s = K$ is often used (see, e.g., [1, 13–15]). In most cases, the coefficient K is assumed to be equal to unity. However, Rickett [1] notes that this coefficient depends on the shape of the autocorrelation function and on the transfer functions of the medium and, only for a thin phase screen with a Gaussian spectrum of inhomogeneities, it may be assumed that $K = 1$. The 6th column of Table 1 gives the values of K_1 obtained as a result of numerical simulation for various shapes of a given frequency profile of spectral distortions, assuming that we managed somehow to measure the true widths of the frequency profile and the true value of $\Delta\tau_s$, e.g., by analyzing the scattered average profile. It can be seen that, even in this ideal experiment, the coefficient K_1 is close to unity only for the shape of the frequency profile in the form of a two-sided exponential, which was noted in Section 2. In the general case, the coefficient K_1 varies from 0.124 to 1.66. The last column of Table 1 gives the calculated values of the coefficient K_2 for a more realistic case when $\Delta\tau_s$ are determined by measuring the pulse broadening and Δf is taken as the half width of the frequency cross section of the ACF. In this variant, K_2 varies from 1.15 to 2.35. It is this variant that is often used to convert the measured pulse broadening time $\Delta\tau_s$ into the decorrelation band Δf and vice versa.

Let us consider, for example, the values of $\Delta\tau_s$ presented in the Australian catalog of pulsars [16], which were obtained in two ways: (1) by measuring the broadening of the average pulse profile due to scattering and (2) by recalculating from Δf measured from the frequency correlation function, using the uncertainty relation $2\pi\Delta f\Delta\tau_s = K$ with $K = 1$. Figure 3 shows the dependence of $\Delta\tau_s$ on the dispersion according to the Australian catalog [16]. In the figure, two zones are distinguished, separated by a dotted line at $\Delta\tau_s = 10$ μs. Greater values of $\Delta\tau_s$ were determined from pulse broadening measurements, while smaller values were obtained by the recalculation from Δf. However, from our analysis, it follows that the value K is on average approximately 2! This means that the recalculated values of $\Delta\tau_s$ are reduced by about 2 times. In our opinion, this explains the observed violation of the continuous distribution of points in the figure.

5. CONCLUSIONS

When estimating the main parameters of pulsar radio emission scattering by inhomogeneities of the interstellar plasma Δf (decorrelation band) and t_{scint} (characteristic scintillation time), it is customary to measure them from the half widths of the frequency and time autocorrelation functions taken at the level 1/2 and $1/e$, respectively. This is convenient when comparing the results obtained by different authors in different epochs and at different frequencies. The numerical simulation performed in this work indicates that the estimates of the scintillation parameters from the autocorrelation functions give values that are shifted with respect to the true characteristics of the scattering processes, namely, the values of decorrelation band Δf overestimated on average 3-fold and the values of the scintillation time t_{scint} overestimated 2-fold. Such significant overestimations of the parameters can be of significant importance when constructing statistical relations and when comparing observations with theoretical predictions. To convert the measured ACF parameters to the true values, we recommend approximating the ACF cross sections using the universal exponential function $U(x)$ (6), measure the half width of this function $W^U_{1/e} = b^{1/m}$, to find from the value of the exponent m_1 (the second column of Table 1) the corresponding factor R of the broadening of the ACF (fourth column of Table 1), and get an estimate of the true value of the parameter $W^{\text{cor}}_{1/e} = W^{\text{obs}}_{1/e}/R$.

To convert from the values of the decorrelation band Δf to the pulse broadening $\Delta\tau_s$ due to scattering (and vice versa), the relation $2\pi\Delta f\Delta\tau_s = K$ is commonly used. In most cases, it is assumed that $K = 1$. Rickett (1977) remarked that K may theoretically depend on the transfer function of the medium. In Table 1, the last two columns give the values of the coefficients K_1 and K_2 for the ideal case of measurements (K_1) and for real conditions of the conversion from the decorrelation bandwidth Δf measured from the ACF cross section to the pulse broadening $\Delta\tau_s$ in time. If the frequency cross section of the ACF was approximated by a universal exponential function $U(x)$, then one can choose the value of K_2 in the corresponding row of Table 1. On average, the value of the factor is $K_2 = 2.2$.

CONFLICT OF INTEREST

The authors declare that they have no conflicts of interest.

REFERENCES

1. B. J. Rickett, Ann. Rev. Astron. Astrophys. **15**, 479 (1977).
2. J. M. Cordes, J. M. Weisberg, and V. Boriakoff, Astrophys. J. **288**, 221 (1985).
3. J. M. Cordes, Astrophys. J. **311**, 183 (1986).
4. N. D. R. Bhat, A. P. Rao, and Y. Gupta, Astrophys. J. Suppl. **121**, 483 (1999).
5. A. D. Kuzmin and B. Ya. Losovsky, Astron. Astrophys. Trans. **26**, 597 (2007).
6. V. V. Andreyanov, N. S. Kardashev, and V. V. Khartov, Cosmic Res. **52**, 319 (2014).
7. M. V. Popov, N. Bartel, M. S. Burgin, C. R. Gwinn, T. V. Smirnova, and V. A. Soglasnov, Astrophys. J. **888**, 57 (2020).
8. V. I. Shishov, Sov. Astron. **17**, 598 (1974).
9. J. M. Armstrong and B. J. Rickett, Mon. Not. R. Astron. Soc. **194**, 623 (1981).
10. A. Wolszczan, Mon. Not. R. Astron. Soc. **204**, 591 (1983).
11. W. Feller, *An Introduction to Probability Theory and its Application,* 2nd ed. (Wiley, New York, 1971), Vol. 2.
12. M. V. Popov and T. V. Smirnova, Astron. Rep. **65**, 1129 (2021).
13. O. B. Slee, G. A. Dulk, and R. E. Otrupchek, Proc. Astron. Soc. Austral. **4**, 100 (1980).
14. J. M. Sutton, Mon. Not. R. Astron. Soc. **155**, 51 (1971).
15. D. C. Backer, Astrophys. J. **190**, 667 (1974).
16. R. N. Manchester, G. B. Hobbs, A. Teoh, and M. Hobbs, Astron. J. **129**, 1993 (2005).

Translated by E. Chernokozhin

SPELL: OK